

Cancer Cell, Volume 16

Supplemental Data

AKT-Independent Signaling Downstream of Oncogenic

PIK3CA Mutations in Human Cancer

Krishna M. Vasudevan, David A. Barbie, Michael A. Davies, Rosalia Rabinovsky, Chontelle J. McNear, Jessica J. Kim, Bryan T. Hennessy, Hsiuyi Tseng, Panisa Pochanard, So Young Kim, Ian F. Dunn, Anna C. Schinzel, Peter Sandy, Sebastian Hoersch, Qing Sheng, Piyush B. Gupta, Jesse S. Boehm, Jan H. Reiling, Serena Silver, Yiling Lu, Katherine Stemke-Hale, Bhaskar Dutta, Corwin Joy, Aysegul A. Sahin, Ana Maria Gonzalez-Angulo, Ana Lluch, Lucia E. Rameh, Tyler Jacks, David E. Root, Eric S. Lander, Gordon B. Mills, William C. Hahn, William R. Sellers, and Levi A. Garraway

Cancer Cell
Supplemental Data for

**AKT-independent signaling downstream of oncogenic
PIK3CA mutations in human cancer**

Krishna M. Vasudevan,* David A. Barbie,* Michael A. Davies,* Rosalia Rabinovsky, Chontelle J. McNear, Jessica J. Kim, Bryan T. Hennessy, Hsiuyi Tseng, Panisa Pochanard, So Young Kim, Ian F. Dunn, Anna C. Schinzel, Peter Sandy, Sebastian Hoersch, Qing Sheng, Piyush B. Gupta, Jesse S. Boehm, Jan H. Reiling, Serena Silver, Yiling Lu, Katherine Stemke-Hale, Bhaskar Dutta, Corwin Joy, Aysegul A. Sahin, Ana Maria Gonzalez-Angulo, Ana Lluch, Lucia E. Rameh, Tyler Jacks, David E. Root, Eric S. Lander, Gordon B. Mills, William C. Hahn, William R. Sellers, and Levi A. Garraway[†]

[†]To whom correspondence should be addressed. Email: levi_garraway@dfci.harvard.edu

*These authors contributed equally to this work.

This file includes:

Supplemental Experimental Procedures

Supplemental References

Figures S1 through S9

Tables S1 through S3

Supplemental Experimental Procedures

Immunoblot Analysis, Transfections and Fluorescence Microscopy. Cells were harvested, washed with PBS and lysed in 150 mM TNN lysis buffer [(50 mM Tris (pH 7.4), 0.5% NP40, 150 mM NaCl, 1 mM NaF, 1 mM Na₃VO₄, 5 mM EDTA (pH 8.0) supplemented with complete Protease Inhibitor Cocktail tablet (Roche)] for 30 min on ice. Lysates were centrifuged at 14,000 rpm for 10 min and protein concentration in the supernatant was determined by the Bradford method (Pierce, Rockford, IL). Equal amounts of total protein were resolved by SDS-PAGE and transferred onto nitrocellulose membranes. Blots were probed overnight at 4° C with antibodies against the proteins of interest. After incubation with horseradish peroxidase-conjugated secondary antibodies, proteins were detected using chemiluminescence (Pierce).

For antibody-based immunofluorescence studies, cells were seeded on sterile glass chamber slides (Lab-Tek II – Nalge Nunc International, Naperville IL). In some cases, cells were also serum-starved for 24 hours and/or treated with either 20 μM LY294002 (or vehicle) for 6 hours. Subsequently, cells were washed in PBS, fixed for 20 min in 4% paraformaldehyde, and permeabilized with 0.5% saponin in PBS for 15 min. Cells were then blocked for 1 hour in 10% goat serum (Sigma) and incubated with the primary antibody overnight at 4° C in PBS. After washing, incubation with a secondary antibody was carried out for 1 hour at 37° C using 10% goat serum in PBS. The following antibodies were used: anti-AKT1 mouse monoclonal antibody (2H10; Cell Signaling Technology), anti-PtdIns(3,4,5)P₃ mouse monoclonal antibody (Z-P345b) (Echelon Biosciences), and Alexa Fluor 594 F(ab')₂ fragment of goat anti-mouse IgG secondary antibody (Cat. #. A11020) (Invitrogen, Molecular Probes, Eugene, Oregon). Cells were counterstained with DAPI-containing mounting medium Vectashield (Vector Laboratories) and examined using a fluorescent microscope (Olympus; 200 × magnification).

To perform GFP immunofluorescence studies, cells were transfected with the indicated GFP-fusion proteins or control GFP vectors in 6 well plates using Lipofectamine 2000 reagent according to the manufacturer's protocol. 48 hrs after transfection, live cells were visualized using a fluorescent microscope to determine subcellular localization of GFP fusion proteins.

Virus Production, Titration and Infection. Lentiviruses were produced by transfection of 293e cells with the packaging plasmids encoding $\Delta 8.9$ and VSV-G, along with the lentiviral shRNA vector using Lipofectamine 2000 reagent, according to the manufacturer's instructions. Culture supernatants containing lentivirus were collected 48 hr post-transfection. These supernatants were passed through 0.45 μm SFCA membrane filters (Nalgene) and supplemented with 10 $\mu\text{g/ml}$ polybrene (Sigma). Lentiviral supernatants were then titrated to reduce nonspecific viral cytotoxicity using NIH 3T3 cells. For titration, 1×10^5 cells were plated in 6 well plates and infected with serial dilutions of viral supernatant (1.5 ml/well, in duplicate). 48 h after infection, one set of infected cells was selected with puromycin and the other set was left unselected. Three days later, cells from both selected and unselected populations were enumerated (Coulter counter) and the ratio of surviving cells in puromycin selected cells versus unselected cells was determined. Viral titers that yielded a 50% cell survival ratio were used for subsequent infections.

To perform lentiviral infections, the target cells were plated at 40-50% confluence and incubated overnight (16 hr). On the day of infections, the culture medium was replaced by the appropriately titered viral supernatant (1.5 ml/well) and incubated at 37° C for 10 hours; afterwards, the viral supernatant was replaced with fresh media. Forty-eight hrs later, infected cell populations were selected in puromycin (2 $\mu\text{g/ml}$): After 5 days of selection, knock down efficiency was determined by Western blot analysis for respective proteins with specific antibodies.

Reverse Phase Protein Lysate Array (RPPA Studies). For RPPA assays, cells or tumors were lysed in RPPA lysis buffer (1% Triton X-100, 50mM HEPES, pH 7.4, 150mM NaCl, 1.5mM MgCl₂, 1mM EGTA, 100mM NaF, 10mM Na Pyrophosphate, 1mM Na₃VO₄, 10% glycerol, 1mM PMSF and 10 $\mu\text{g/ml}$ aprotinin). Samples were incubated on ice for 20-30 minutes and centrifuged at 14,000 rpm. Protein concentration in the resulting supernatant was determined by the Bradford method (Pierce, Rockford, IL). After dilution to 1 mg/ml concentration, lysates were boiled in 1% SDS. Five serial dilutions were prepared for each lysate on 96-well plates using additional lysis buffer with 1% SDS, and samples were transferred to 384-well plates. Protein was then spotted onto nitrocellulose-coated glass slides (FAST Slides, Schleicher &

Schulee Bioscience, Inc., Keene, NH) using an automated GeneTac Arrayer (Genomic Solutions, Inc., Ann Arbor, MI). Slides were stored at -20° C after printing.

To detect protein levels, the RPPA slides were first blocked for endogenous peroxidase, avidin, and biotin protein activity; slides were then incubated with primary and secondary antibodies as described previously (Tibes et al., 2006). Antibodies for p-AKT S473, p-AKT T308, p-GSK3 α/β S21/9, p-TSC2 T1462, p-PDK1 S241, and PTEN were purchased from Cell Signaling Technology (Danvers, MA). The antibody signal was amplified using a DakoCytomation-catalyzed detection system (Carpinteria, CA). The stained slides were scanned, analyzed, and quantitated using Microvigen software (VigeneTech Inc., North Billerica, MA) to generate a serial dilution-signal intensity “supercurve” for all samples on the slide. Each sample was then fitted to this “supercurve” to generate logarithmic values representative of relative signal intensity. Differences in protein loading were determined using the median expression level for each sample across all antibodies used (additional antibodies, which varied by experiment, are listed in Supplemental Methods); protein values were divided by this factor. These corrected values were used for statistical analysis.

PIK3CA Mutation Detection in Human Breast Tumors. MALDI-TOF mass spectrometry-based SNP detection was performed using a Sequenom MassARRAY (San Diego, CA). Analysis was performed to detect the E17K-AKT1 mutation, mutations in the equivalent sites of AKT2 and AKT3 and 26 known mutations in PIK3CA (PIK3CA_A1046V, PIK3CA_C420R, PIK3CA_E110K, PIK3CA_E418K, PIK3CA_E453K, PIK3CA_E542K, PIK3CA_E545K, PIK3CA_F909L, PIK3CA_G1049R, PIK3CA_G451L456_V, PIK3CA_H1047L, PIK3CA_H1047R, PIK3CA_H1047Y, PIK3CA_H701P, PIK3CA_K111N, PIK3CA_M1043V, PIK3CA_N345K, PIK3CA_P539R, PIK3CA_Q060K, PIK3CA_Q546E, PIK3CA_R088Q, PIK3CA_S405F and PIK3CA_T1025S (Ding et al., 2004; Jurinke et al., 2002 and Thomas et al., 2007). Genomic DNA flanking the designated mutation (SNP) was amplified by PCR, and excess primers and nucleotides were removed using EXO-SAP (Sequenom). Next, primer extension reactions were performed using the Sequenom iPLEX protocol. The iPLEX reactions were then desalted (Clean Resin; Sequenom) and spotted onto Spectrochip matrix chips using a Samsung Nanodispenser. The chips were analyzed using the MassArray (Sequenom). All spectra

were generated in duplicate and visually inspected to confirm allele calls. Reactions in which > 15% of product mass corresponded to the mutant variant in both reactions were scored as positive. All E17K-AKT1 mutations were confirmed with independent primers and Sanger sequencing in the MDACC CCSG-supported sequencing core (results were concordant in all cases).

PTEN Sequencing in Human Breast Tumors. A high-throughput approach to the resequencing of *PTEN* and *PIK3CA* was performed on the breast tumor specimens following whole genome amplification (Tartaglia et al., 2007). The resequencing protocol was as follows: oligonucleotide primers (sequences available upon request) for amplifying the relevant *PIK3CA* coding exons were designed to yield a product size of 200–700 bp, with a minimum of 40 bp flanking the splice sites. Primer design was carried out using the Exon Primer program (UCSC Genome Browser, build hg17). M13F and M13R tags were added to the forward and reverse primers, respectively. Five nanograms of genomic DNA from each breast tumor were amplified in an 8- μ l PCR reaction using AmpliTaq Gold (Applied Biosystems) on PE 9700 machines and cleaned using a diluted version of the Exo-SAP based PCR product pre-sequencing kit (USB Corporation), dispensed by a nanoliter dispenser (Deerac Fluidics Equator). PCR procedures were performed in a 384-well format using a Biomek NX workstation after optimization. Sequencing reactions were performed using the M13 primers and the BigDye Terminator v3.1 Cycle Sequencing Kit (Applied Biosystems); products were cleaned with BET before separation on an ABI 3730xl DNA Analyzer. Base calling, quality assessment and assembly were carried out using the Phred, Phrap, Polyphred, and Consed software suites. All sequence variants were verified by manual inspection of the chromatograms, and putative causative mutations were verified by independent sequencing reactions. Mutation frequencies determined by this approach may represent underestimates, as all exon sequences were not covered in all subjects with perfect mutation capture. In contrast, the false-positive rate with this approach is low (Tartaglia et al., 2007).

Anchorage Independent Growth Assays. 5×10^4 cells were seeded in 6 well plates, with a bottom layer of 0.5% Noble agar in RPMI and a top layer of 0.4% Noble agar-containing RPMI. Fresh RPMI (0.5 ml) containing puromycin was added after 1.5 weeks to retain adequate

hydration. After 4 weeks, colonies were stained with Iodonitrotetrazolium chloride (Sigma) for 12 hrs. Enumeration of soft agar colonies was performed as described elsewhere (Lee et al., 2006). Colonies were counted using ten random images (40× magnification) from each well. Colonies from three replicate wells were enumerated, with the mean and standard deviation represented graphically (see text).

Cell Proliferation Assay. 3×10^4 cells per well were plated in 12 well plate in triplicate and cells in each well were counted using Vi-CELL XR cell counter at every 24 hours upto 144 hours. The average cell numbers from triplicate wells with standard deviation were shown.

References

Ding, C., Chiu, R.W., Lau, T.K., Leung, T.N., Chan, L.C. *et al.* (2004). MS analysis of single-nucleotide differences in circulating nucleic acids: Application to noninvasive prenatal diagnosis. *Proc. Natl. Acad. Sci. U S A.* *101*, 10762-7.

Jurinke, C., van den Boom, D., Cantor, C.R., Köster, H. (2002). Automated genotyping using the DNA MassArray technology. *Methods Mol. Biol.* *187*, 179-92.

Tartaglia, M., Pennacchio, L.A., Zhao, C., Yadav, K.K., Fodale, V., Sarkozy, A., Pandit, B., *et al.* (2007). Gain-of-function SOS1 mutations cause a distinctive form of Noonan syndrome. *Nat Genet.* *39*, 75-9.

Thomas, R.K., Baker, A.C., DeBiasi, R.M., Winckler, W., Laframboise, T., Lin, W.M., Wang, M., *et al.* (2007). High-throughput oncogene mutation profiling in human cancer. *Nat Genet.* *39*, 347-51.

Tibes, R., Qiu, Y., Lu, Y., Hennessy, B., Andreeff, M., Mills, G. B., and Kornblau, S. M. (2006). Reverse phase protein array: validation of a novel proteomic technology and utility for analysis of primary leukemia specimens and hematopoietic stem cells. *Mol Cancer Ther* *5*, 2512-2521.

Figure S1

Breast Cancer Cell Lines

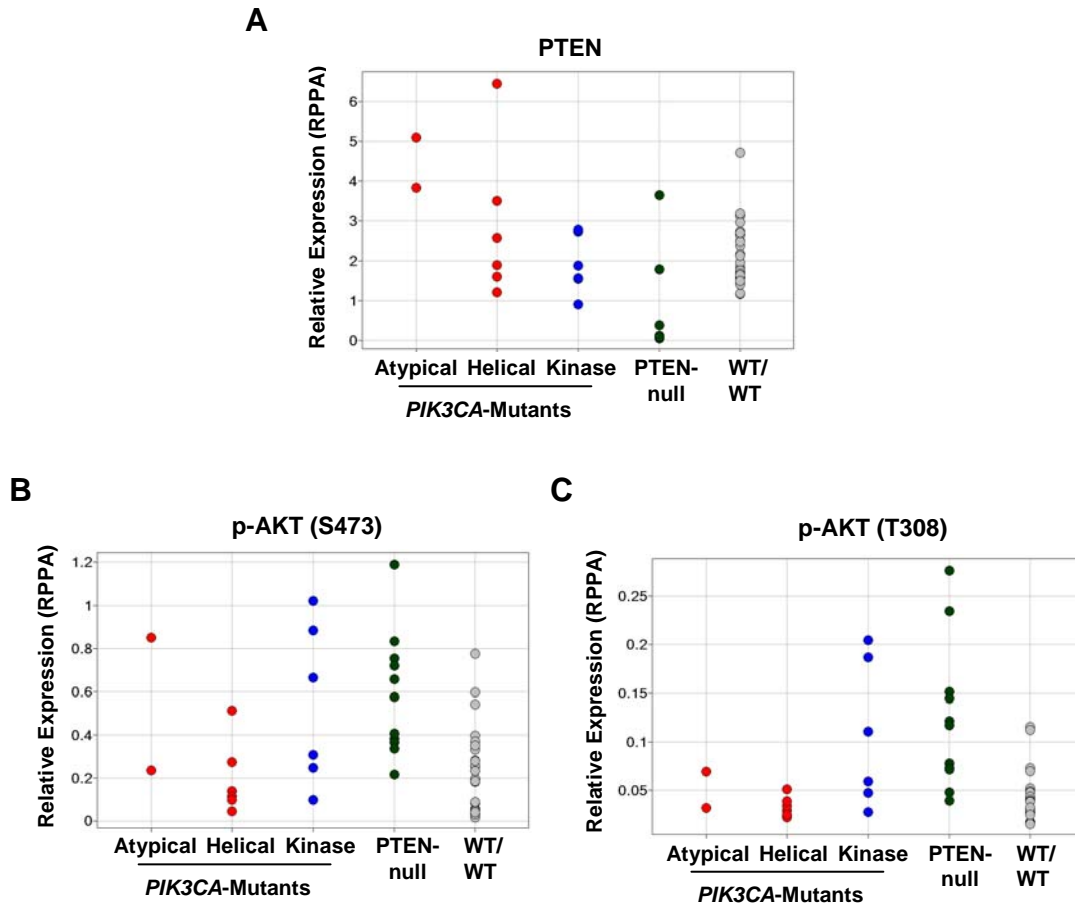


Figure S1. RPPA analysis of 51 human breast cancer cell lines. Scatter plots of PTEN (A) p-AKT (S473) (B) or p-AKT (T308) (C) RPPA expression are shown for 51 human breast cancer cell lines. Cell lines are classified by *PIK3CA* mutation type as follows: Atypical (somatic *PIK3CA* mutations outside of the helical or kinase domains; in this case K111N and N345K), Helical (E545K or E542K), or Kinase (H1047R) mutations. Cells with PTEN protein loss or known inactivating mutations were classified as PTEN-null; those with no known abnormalities for either *PIK3CA* or PTEN were classified as Wild-Type (WT). As in the NCI60 panel, cell lines with PTEN loss have higher levels of p-AKT (Ser473) and p-AKT (Thr308) as compared to WT cells ($p < 0.001$ for both residues). Cell lines with helical *PIK3CA* mutations have significantly lower p-AKT (Ser473) ($p = 0.03$) and p-AKT (Thr308) ($p = 0.02$) levels than those with PTEN loss.

Figure S2

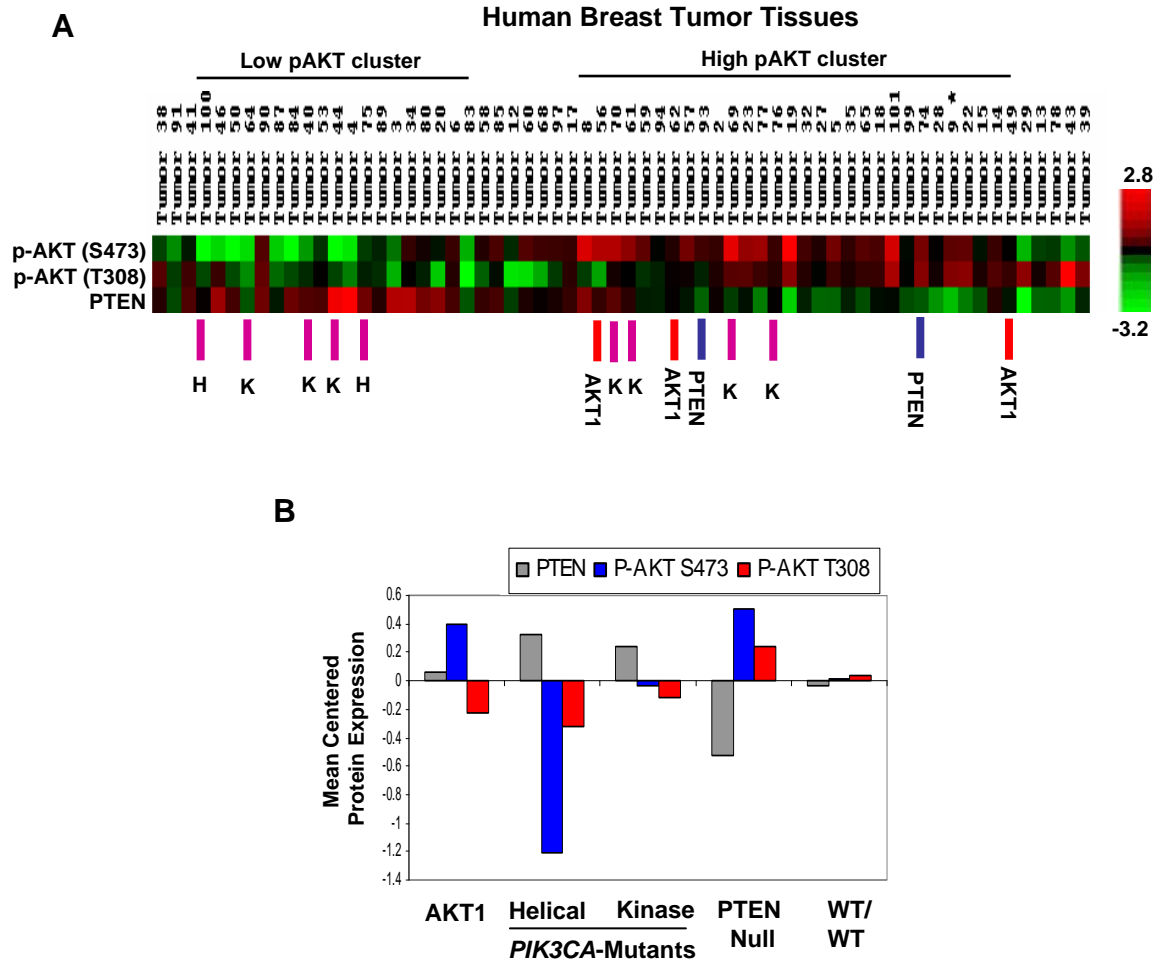


Figure S2. PTEN-null and *PIK3CA*-mutant breast tumors show different steady-state AKT pathway activation patterns. (A) Unsupervised hierarchical clustering of p-AKT (S473 and T308) and PTEN expression, as determined by RPPA, in 64 hormone receptor positive breast tumors from patients. Samples with mutations in PTEN, *AKT1*, *PIK3CA* helical (H) or *PIK3CA* kinase domains (K) are indicated. (B) Quantitative RPPA protein expression of PTEN and p-AKT in 64 hormone receptor-positive breast tumor samples. The average of the mean-centered protein expression levels of PTEN (gray bars), P-AKT Ser473 (blue bars), and P-AKT Thr308 (red bars) for tumors with each mutation is shown.

Figure S3

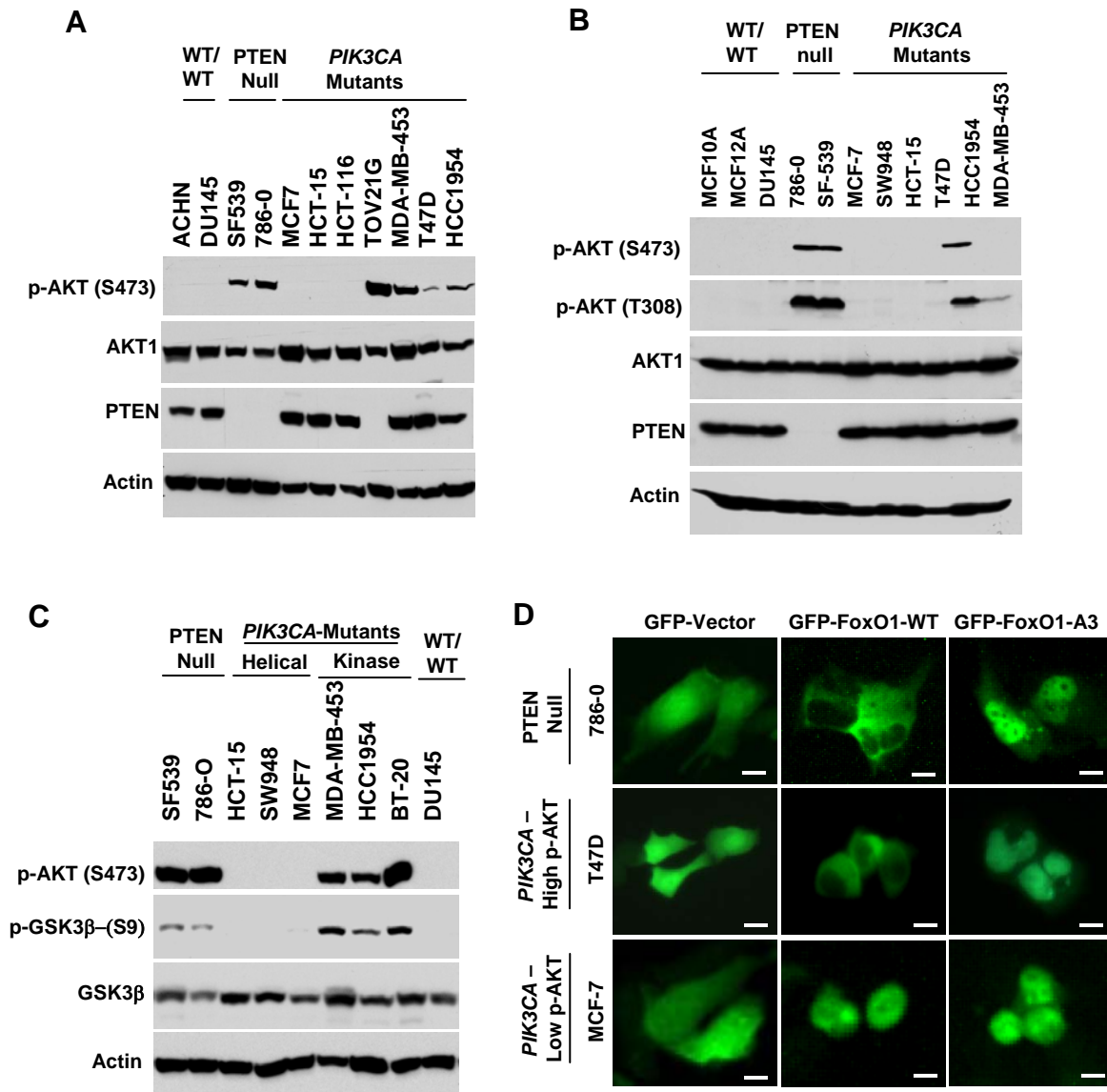


Figure S3. AKT phosphorylation and downstream pathway activation is decreased in some *PIK3CA*-mutant cell lines. (A) Immunoblot studies of p-AKT (S473), total AKT1, PTEN and Actin in selected PTEN-null and *PIK3CA*-mutant cell lines. *PIK3CA*-mutant lines with both helical (MCF-7 and HCT-15) and kinase domain mutations (HCT-116) may show low p-AKT. (B) Immunoblot analysis of selected PTEN-null and *PIK3CA*-mutant cell lines under serum-starved conditions. (C) Immunoblot analysis of phospho-GSK3β (S9) as in relation to AKT phosphorylation (S473) and PTEN or *PIK3CA* mutation status (top). (D) FoxO1 localization studies in *PIK3CA*-mutant cells. Transiently transfected GFP (control; left column), GFP-FOXO1 (middle column), or GFP-FOXO1-A3 (resistant to cytoplasmic retention; right column) constructs were examined in PTEN-null cells (786-0), *PIK3CA*-mutant cells with high p-AKT (T47D), and *PIK3CA*-mutant cells with low p-AKT (MCF-7). Scale bars = 30 μM.

Figure S4

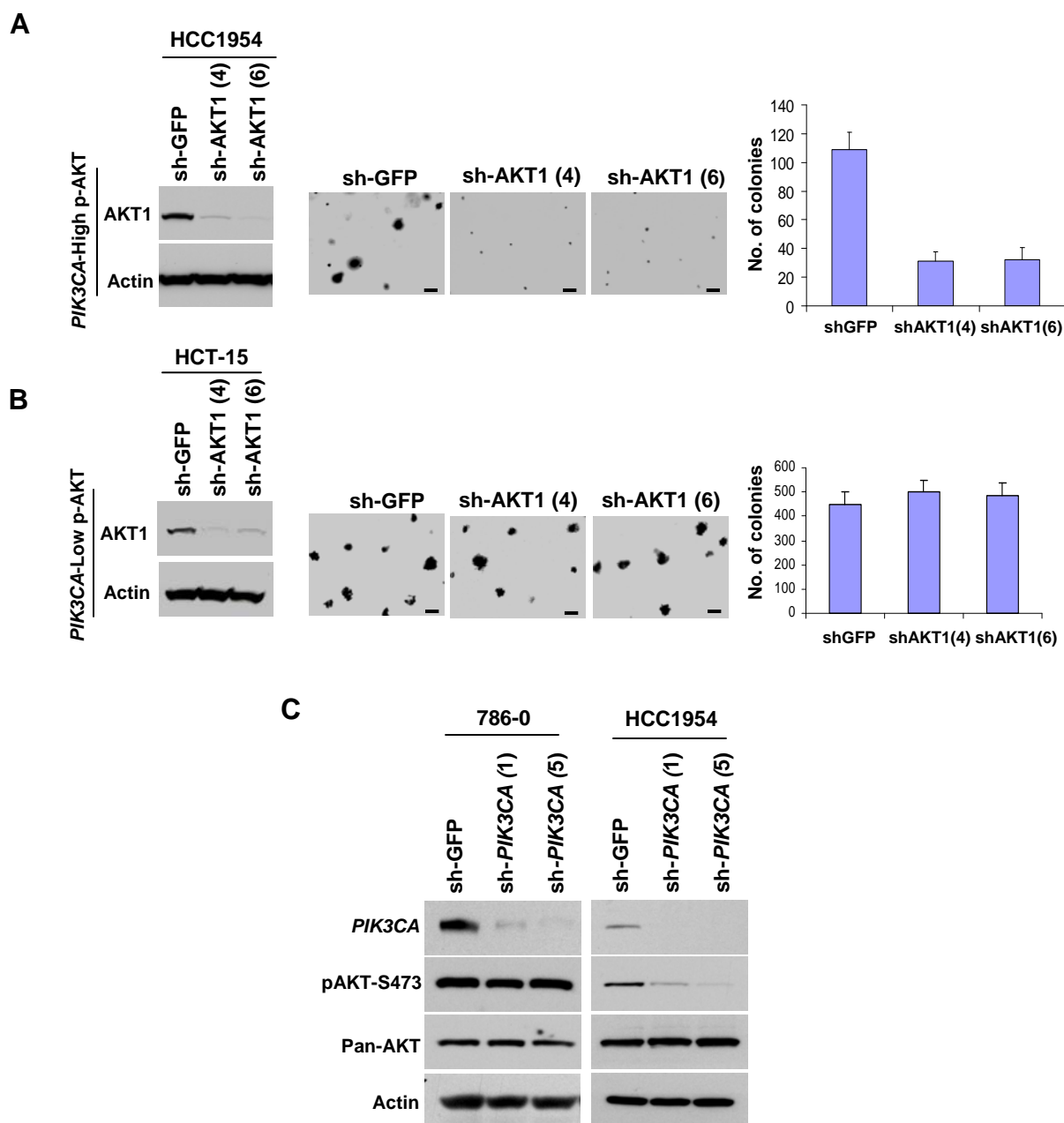


Figure S4. Effect of AKT knockdown in *PIK3CA*-mutant cells. Anchorage-independent growth following lentiviral RNAi knockdown of *AKT1* in HCC1954 (*PIK3CA*^{kinase}) (A) and HCT-15 (*PIK3CA*^{helical}) (B) cells is shown. Knockdown efficacy of two independent shRNAs was measured by Western blot (left), and colony formation in soft agar was measured and enumerated (bar graphs; right). Data are mean \pm SD; each experiment was performed in triplicate. Scale bars = 600 μ M. (C) *PIK3CA* knockdown results in decreased p-AKT (S473) levels in the HCC1954 cell line (*PIK3CA*^{kinase}) but not in the 786-0 cell line (PTEN-null).

Figure S5

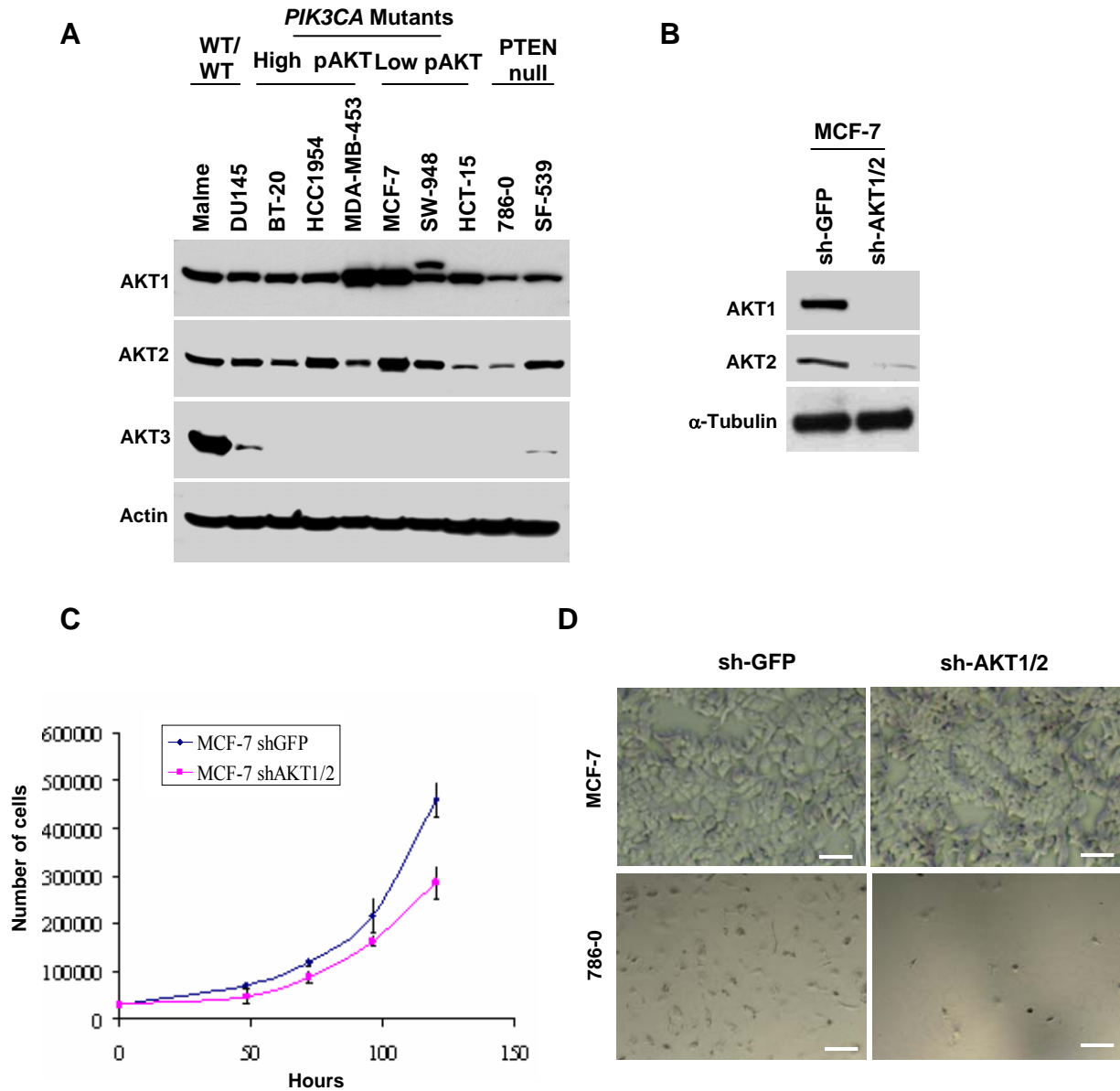


Figure S5. AKT isoform expression and combined knockdown studies. (A) Immunoblot studies of AKT isoforms (AKT1, AKT2, and AKT3) in selected PTEN-null and *PIK3CA*-mutant cell lines. Most cancer cell lines examined express both AKT1 and AKT2; MALME (melanoma), DU-145 (prostate) and SF-539 (CNS) also express AKT3. (B) Combined knockdown of AKT1 and AKT2 in MCF-7 cells (*PIK3CA*-mutant, low p-AKT). (C) MCF-7 cell proliferation following infection and puromycin selection using control (shGFP) or a combination of lentiviral constructs targeting AKT1 and AKT2 (shAKT1/2). Data are mean \pm SD; each experiment was performed in triplicate. (D) Effects of control (shGFP) or combined AKT1 and AKT2 knockdown (shAKT1/2) on cell growth in MCF-7 cells (*PIK3CA*-mutant, low p-AKT) or 786-0 cells (PTEN-null, high p-AKT). Combined AKT1/2 knockdown was markedly deleterious in 786-0 cells but had only minimal effects on MCF-7 cell growth. Scale bars = 300 μ M.

Figure S6

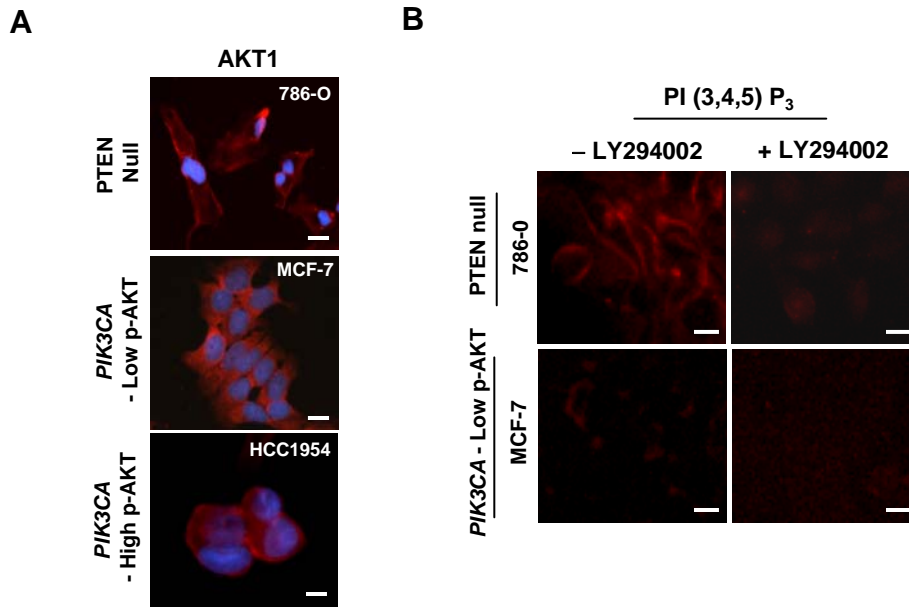


Figure S6. AKT localization and membrane phosphatidylinositides in PTEN null and *PIK3CA*-mutant cells. (A) Immunofluorescence studies of AKT1 localization (red) and DAPI nuclear staining (blue) are shown for PTEN-null (786-0), *PIK3CA*-mutant, low p-AKT (MCF-7) and *PIK3CA*-mutant, high p-AKT (HCC1954) cells. Scale bars = 30 μ M. (B) The effect of LY294002 (20 μ M) treatment on phosphatidylinositide immunofluorescence is shown for 786-0 or MCF7 cells. A monoclonal antibody recognizing PtdIns (3,4,5) P₃ was used for this experiment. Scale bars = 30 μ M.

Figure S7

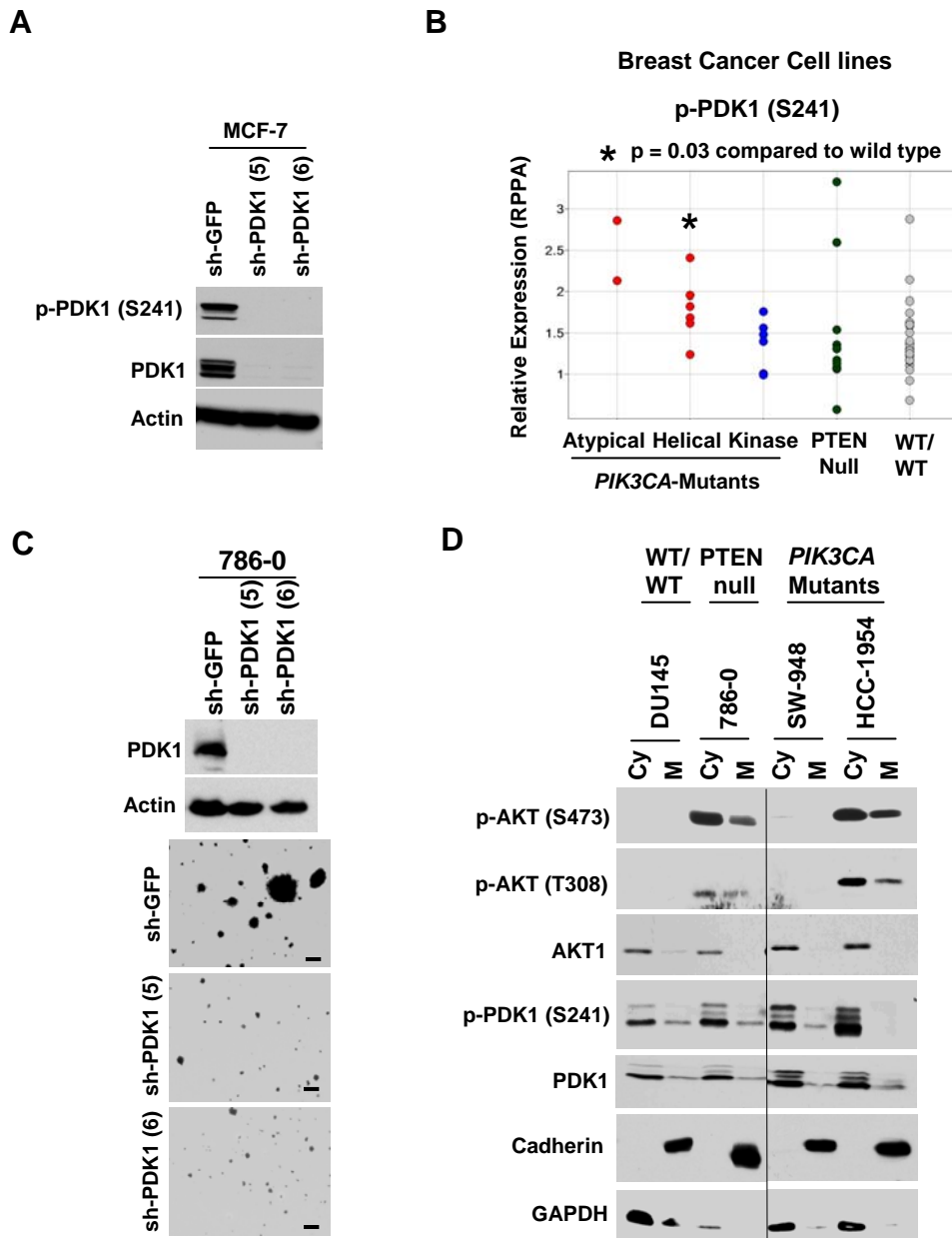


Figure S7. Biochemical and functional studies of PDK1. (A) Lentiviral shRNA knockdown of PDK1 (2 independent shRNAs) confirms the identify of proteins recognized by p-PDK1(S241) and total PDK1 antibodies. (B) Scatter plot of p-PDK1 (S241) expression in 51 human breast cancer cell lines, as determined by RPPA. Analyses of p-AKT and PTEN for the same cell lines are shown in Fig.S1D-F. (C) Anchorage-independent growth following lentiviral RNAi knockdown of PDK1 in 786-0 (PTEN-null) cells is shown. Knockdown efficacy of two independent shRNAs was measured by Western blot (top), and colony formation in soft agar was measured. Scale bars = 600 μ M. (D) Additional immunoblotting studies of cytosolic (Cy) and membrane (M) fractions to those in the main text are shown, including “wild-type” (DU-145), PTEN-null (786-0), or $PIK3CA$ -mutant cells (SW-948 and HCC-1954).

Figure S9

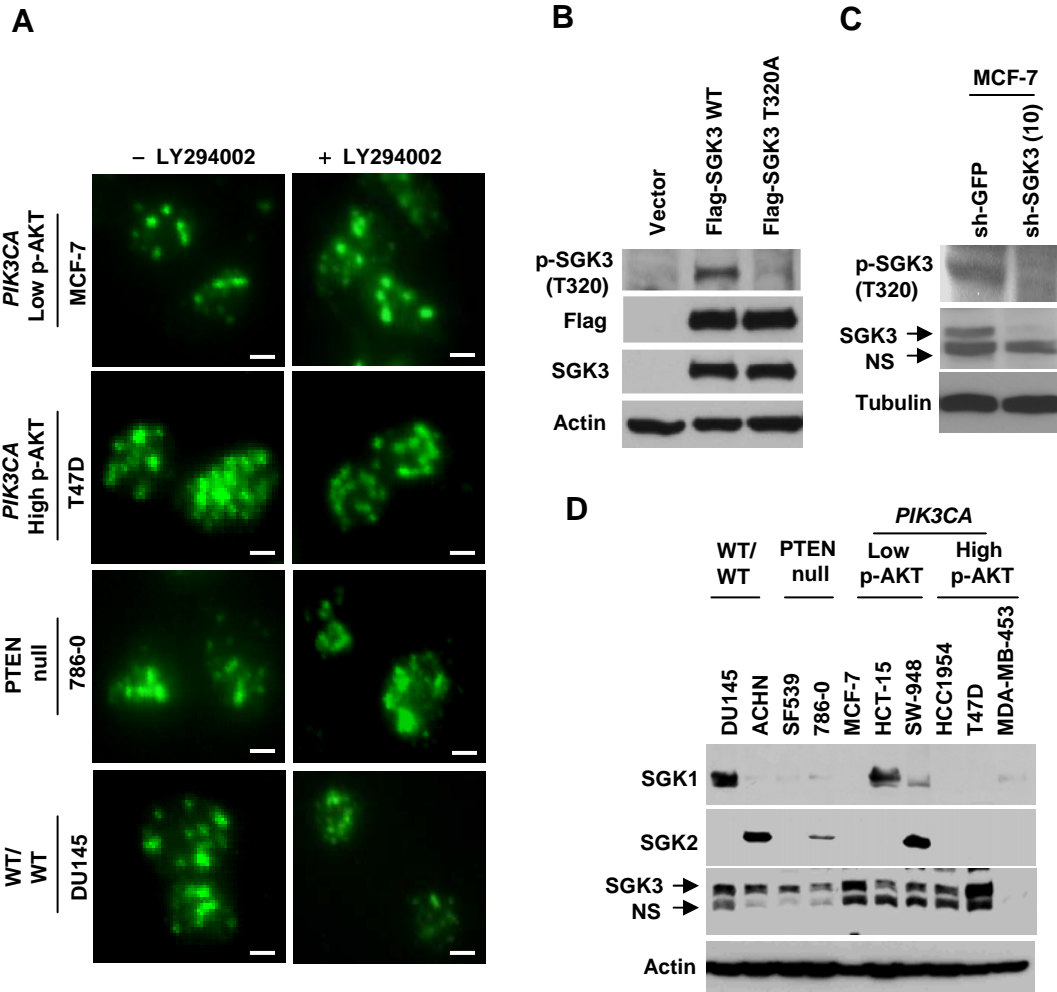


Figure S9. SGK3 localization and SGK isoform expression in *PIK3CA*-mutant cells.

(A) Cellular localization of a transiently transfected GFP-PX-SGK3 construct was examined in the absence (left panel) or presence of LY294002 (20 μ M for 2 hours) (right panel) in *PIK3CA*-mutant cells with low p-AKT (MCF-7), *PIK3CA*-mutant cells with high p-AKT (T47D), PTEN-null cells (786-0) and wild-type cells (DU145). Scale bars = 30 μ m. (B and C) Immunoblot analysis confirms recognition of SGK3 phosphorylation at Thr320 by a polyclonal antibody (Cell Signaling Technology, special order), based on ectopic expression of epitope-tagged wild-type (Flag-SGK3-WT) or Thr320-mutated (Flag-SGK3 T320A) variant (B) and based on knock-down of endogenous SGK3 (C) in MCF-7 cells. (D) Immunoblot studies of SGK isoforms (SGK1, SGK2, and SGK3) in selected PTEN-null and *PIK3CA*-mutant cell lines (NS – Non specific band). Most cancer cell lines examined express SGK3, whereas only a few express SGK1 or SGK2.

Supplemental Table 1
Cell Lines for the RNAi Screen

Cell Lines	PIK3CA Mutation	p-AKT Status
T47D	H1047R (kinase domain)	High
MDA-MB-453	H1047R (kinase domain)	High
TOV21G	H1047R (kinase domain)	High
HCT-116	H1047R – (kinase domain)	Low
MCF-7	E545K – (helical domain)	Low
DLD1/HCT-15	E545K – (helical domain)	Low

Supplemental Table 2
PDK1 Substrates Used for RNAi Screen

Gene	Protein
AKT1	AKT1
AKT2	AKT2
AKT3	AKT3
PRKCA	PKA
PRKCB1	PKC-beta
PRKCD	PKC-Delta
PRKCI	PKC-iota
PRKCG	PKC-gamma
PRKCZ	PKC-zeta
PKN1	PKV-like 1
PKN2	PKC- like 2
RPS6KA1	p90-RSK1
RPS6KA2	p90-RSK3
RPS6KA3	p90-RSK2
RPS6KA4	p90-RSK, polypeptide 4
RPS6KA5	p90-RSK, polypeptide 5
RPS6KB1	p70-S6K1
RPS6KB2	p70-S6K2
SGK2	SGK2
SGK3	SGK3

Supplemental Table 3**List of shRNA constructs used for the functional study**

Clone ID	Gene ID	Symbol	Sequence	shRNA name	Label in Figs.
TRCN0000196501	NM_001033578	SGK3	GTTTCATGGTATGATCGAAATG	shSGK3-2103	shSGK3(5)
TRCN0000001521	NM_001033578	SGK3	GCCGAGATGTTGCTGAAATGT	shSGK3-1302	shSGK3(10)
TRCN0000010282	NM_001033578	SGK3	GGCTGAACGTAATGTGCTCTT	shSGK3-838	shSGK3(15)
TRCN0000039603	NM_006218	PIK3CA	GATTCCACACTGCACTGTAA	shPIK3CA-3251	shPIK3CA(1)
TRCN0000010407	NM_006218	PIK3CA	AATGAAAGCTCACTCTGGATT	shPIK3CA-3234	shPIK3CA(5)
TRCN0000039793	NM_005163	AKT1	CGTGCCATGATCTGTATTTAA	shAKT1-1694	shAKT1(1)
TRCN0000039794	NM_005163	AKT1	GATCCTCAAGAAGGAAGTCAT	shAKT1-735	shAKT1(2)
TRCN0000039796	NM_005163	AKT1	GCATCGCTTCTTTGCCGGTAT	shAKT1-1410	shAKT1(3)
TRCN0000039797	NM_005163	AKT1	CGCGTGACCATGAACGAGTTT	shAKT1-628	shAKT1(4)
TRCN0000010163	NM_005163	AKT1	CGAGTTTGAGTACCTGAAGCT	shAKT1-642	shAKT1(6)
TRCN0000010171	NM_005163	AKT1	CTATGGCGCTGAGATTGTGTC	shAKT1-954	shAKT1(7)
TRCN0000010174	NM_005163	AKT1	GGACTACCTGCACTCGGAGAA	shAKT1-981	shAKT1(8)
TRCN0000000563	NM_001626	AKT2	CCCTTAAACAACCTTCTCCGTA	shAKT2-354	shAKT2(1)
TRCN0000000562	NM_001626	AKT2	CGGGCTAAAGTGACCATGAAT	shAKT2-633	shAKT2(2)
TRCN0000010121	NM_002744	PRKCZ	GTTGTTCTGGTCATTGAGTA	shPRKCZ-975	shPRKCZ(1)
TRCN0000010114	NM_002744	PRKCZ	CATGAAAGTGGTGAAGAAAGA	shPRKCZ-837	shPRKCZ(2)
TRCN0000039782	NM_002613	PDPK1	CAAAGTTCTGAAAGGTGAAAT	shPDPK1-1553	shPDK1(5)
TRCN0000001476	NM_002613	PDPK1	GCAGCAACATAGAGCAGTACA	shPDPK1-1306	shPDK1(6)
TRCN0000002745	NM_000314	PTEN	AGGCGCTATGTGTATTATTAT	shPTEN-1548	shPTEN (1)
TRCN0000028991	NM_008960	PTEN	CGACTTAGACTTGACCTATAT	shPTEN-1011	shPTEN(2)
N/A	N/A	GFP	GCAAGCTGACCCTGAAGTTCA	shGFP	shGFP